Extinction of epidemics in lattice models with quenched disorder

S. N. Taraskin*
St. Catharine's College and Department of Chemistry, University of Cambridge, Cambridge, United Kingdom

J. J. Ludlam†
Department of Plant Sciences, University of Cambridge, Cambridge, United Kingdom

C. J. Neugebauer‡
Department of Chemistry, University of Cambridge, Cambridge, United Kingdom

C. A. Gilligan§
Department of Plant Sciences, University of Cambridge, Cambridge, United Kingdom
(Received 25 January 2005; published 18 July 2005)

The extinction of the contact process for epidemics in lattice models with quenched disorder is analyzed in the limit of small density of infected sites. It is shown that the problem in such a regime can be mapped to the quantum-mechanical one characterized by the Anderson Hamiltonian for an electron in a random lattice. It is demonstrated both analytically (self-consistent mean field) and numerically (by direct diagonalization of the Hamiltonian and by means of cellular automata simulations) that disorder enhances the contact process, given the mean values of random parameters are not influenced by disorder.

DOI: 10.1103/PhysRevE.72.016111 PACS number(s): 05.50.+q, 71.23.−k, 02.50.−r

I. INTRODUCTION

The spread of epidemics in complex networks such as biological populations and computer networks is of great current interest, both for practical applications and from a fundamental point of view [1–6].

This is one of the issues of the theory of nonequilibrium phase transitions [1,2] and the theory of complex networks [3,4]. The problems of interest include the question about the existence of a critical regime separating invasive (active) and noninvasive (absorbing) states of the system and, if such a transition exists, how it depends on internal and external parameters and also what the universal features of the transition are (see, e.g., [7]).

In one of the simplest models of epidemics, all the nodes are divided into two classes: infectious (I) and susceptible (S) [8]. The epidemic spreads by a contact process according to which an infected node can transfer infection to another susceptible node with typical infection rate w and recover with typical recovery rate ε becoming again susceptible (the SIS model). The system undergoes a phase transition with variation of the dimensionless parameter, $\eta=w/\varepsilon$, from the absorbing ($\eta<\eta_c$) to active state ($\eta>\eta_c$). The critical value is $\eta_c \sim Z^{-1}$ [3,7], with Z being the typical number of links per node (coordination number).

Usually, the infection and recovery rates are assumed to be node independent. However, in real systems, the values of w and ε can vary from node to node (quenched disorder). Investigations of contact processes in systems with quenched disorder over recent years [1,2,9–17] have resulted in some rather intriguing findings. For example, it has been suggested that the disorder can change the universality class of the model [18,19]. However, the situation is far from being completely understood, and the aim of this paper is to investigate the influence of a general form of quenched disorder on the dynamics of the contact process in the absorbing state. Using a combination of a simple epidemiological model with methods from condensed matter physics, we show how disorder in the infection or recovery rates influences the long-time dynamics (decay time) of epidemics in the absorbing state. This is of practical importance in determining the time to extinction of epidemics within this state. We also identify a lower bound for η_c and show how the degree of disorder influences the magnitude of the extinction rate.

We consider the dynamics of the contact process far in the absorbing state when the problem can be mapped to the quantum-mechanical one described by the disordered Hamiltonian of the Anderson type (see, e.g., [20]) and an approximate method (self-consistent mean field) can be applied. The spectrum of the Hamiltonian under this approximation is then used in the analysis of the long-time dynamics of the system. The advantage of the approach is in the possibility of incorporating a general type of disorder in the analysis while the disadvantage is due to the rather severe restriction of being in the absorbing state (dilute regime for concentration of infected nodes). Our main result is that the disorder slows down the long-time dynamics of the system given that the mean values of the random values stay the same as in ordered systems. The approximate analytical results are supported by exact numerical analysis using a cellular automata approach.

The paper is organized in the following manner. The formulation of the problem is given in Sec. II. The solutions in

*Electronic address: snt1000@cam.ac.uk
†Electronic address: jjl25@cam.ac.uk
‡Electronic address: cjn24@cam.ac.uk
§Electronic address: cag1@cam.ac.uk

the dilute regime both for ordered and disordered cases are presented in Sec. III followed by discussion in Sec. IV. The conclusions are made in Sec. V.

II. FORMULATION OF THE PROBLEM

Consider a set of N nodes (sites) connected to each other by links (infection paths). Each node i can be in one of two states: infected (occupied by an "excitation" and characterized by occupation number $n_i=1$) or not infected (empty with $n_i=0$). The occupation number n_i changes from 0 to 1 as a result of infection from an occupied node j occurring with infection rate w_{ji} and from $n_i=1$ to $n_i=0$ due to natural recovery with rate ε_i. Any state of the system is characterized by the set of occupation numbers, $\{n\}\equiv\{n_1,\ldots,n_N\}$. Bearing in mind the stochastic nature of the infection and recovery processes it is convenient to characterize the system by the state vector $|P(t)\rangle$, the components of which are the probabilities of finding the system in different states at time t, $|P(t)\rangle=|P_{\{n\}}(t)\rangle$, where $n=1,\ldots,2^N$ runs over all the possible states of the system. The time evolution of the state vector is governed by the master equation describing the conserved probability flow [7],

$$\partial_t|P(t)\rangle=\hat{\mathcal{L}}|P(t)\rangle, \tag{1}$$

where $\hat{\mathcal{L}}$ stands for the non-Hermitian Liouville operator, the nonzero elements of which describe the transitions between the states with different numbers of occupied nodes.

It is convenient to make a linear transformation of the state coordinates (change of basis) from $P_{n_1,n_2,\ldots,n_N}$ to the n-site probabilities,

$$\begin{aligned}\bar{P}_i(t)&=\sum_{n_k\neq n_i}P_{n_1,\ldots,n_k,\ldots,n_i,\ldots,n_N}(t),\quad \bar{P}_{ij}(t)\\&=\sum_{n_k\neq n_i,n_j}P_{n_1,\ldots,n_k,\ldots,n_i,\ldots,n_j,\ldots,n_N}(t),\quad \text{etc.},\end{aligned} \tag{2}$$

where $\bar{P}_i(t)$ is the probability of finding node i in an occupied ($n_i=1$) state independent of the occupation of all other nodes. This allows the master equation (1) to be recast in the following form:

$$\partial_t\bar{P}_i(t)=-\varepsilon_i\bar{P}_i(t)+\sum_{j\neq i}w_{ji}[\bar{P}_j(t)-\bar{P}_{ji}(t)], \tag{3}$$

where $\bar{P}_j(t)-\bar{P}_{ji}(t)$ is the probability of finding the system with the occupied jth node and the unoccupied ith node, independent of the state of all other nodes. The single-site probability $\bar{P}_i(t)$ in Eq. (3) is coupled with the double-site probabilities $\bar{P}_{ij}(t)$. A similar probability-balance equation for $\bar{P}_{ij}(t)$ contains the three-site probabilities and so on. This makes the set of simultaneous equations to be coupled and thus be nontrivial for analysis.

The lowest level of approximations in decoupling schemes involves a complete ignorance of the double-site occupations, $\bar{P}_{ij}$, in comparison with other terms in the master equation (3), which is possible if

$$\bar{P}_{ij}(t)\ll\bar{P}_j(t)\ \text{or}\ \bar{P}_{ij}(t)\ll\frac{\varepsilon_i}{w_{ji}}\bar{P}_i(t), \tag{4}$$

for each pair of communicating sites $i-j$ so that the master equation under these approximations transforms to the form

$$\partial_t\bar{P}_i(t)=-\varepsilon_i\bar{P}_i(t)+\sum_j w_{ji}\bar{P}_j(t) \tag{5}$$

and is hereafter referred to as the approximate master equation. The inequalities given by Eq. (4) are valid if the typical recovery rate is much greater than the typical infection rate, $\varepsilon\gg w$, and an epidemic dies out very quickly over the typical time, ε^{-1}. In such a regime, the single-site probabilities are small for the majority of sites practically for all times—i.e., $\bar{P}_i\ll 1$—and this regime can be called a dilute regime for the concentration of infected sites.

Therefore, making approximations given by Eq. (4) we focus on the dynamics of the system far in the absorbing state ($\eta\ll\eta_c$)—i.e., where an epidemic will certainly become extinct. Bearing in mind that the terms $\propto\bar{P}_{ij}$ [entering Eq. (3) with a minus sign] reduce the infection rate due to a possible simultaneous occupation of both communicating sites i and j (the transmission of infection cannot occur between two sites if both of them are already infected) we might expect that the solution of approximate rate equation (5) exhibits the enhancement of an epidemic in the dilute regime. In fact, the approximate master equation (5) on its own describes the spread of an epidemic in the system of N nodes with multiple reinfection of infected nodes where each node can be multiply occupied by the "excitations" (infection) and $\bar{P}_i$ has the meaning of an occupation number which can be larger than 1.

The approximate master equation (5) similarly to the exact one can also have solutions which behave differently as $t\to\infty$ depending on the typical value of the parameter η. In fact, there exists a critical value η_c^* for the approximate master equation which separates the absorbing and active states and this critical value η_c^* is smaller than the critical value η_c for the exact master equation due to the nature of the approximations made. This allows the lower bound estimate, η_c^*, for η_c to be found by solving the approximate problem for a quite general type of disorder.

The state of the system in the dilute regime can be defined in the subspace of the singly occupied sites spanned by the orthonormal site basis $|i\rangle$ and is characterized by the state vector $|\bar{P}\rangle=|\bar{P}_1,\bar{P}_2,\ldots,\bar{P}_N\rangle$ with components $\bar{P}_i(t)=\langle i|\bar{P}(t)\rangle$. The master equation (5) can be recast as

$$\partial_t|\bar{P}(t)\rangle=\hat{\mathcal{H}}|\bar{P}(t)\rangle, \tag{6}$$

where $\hat{\mathcal{H}}$ stands for the Liouville operator which now (under assumption of symmetric infection rates, $w_{ij}=w_{ji}$) is Hermitian and can be associated with the Anderson-like Hamiltonian (see, e.g., [20])

$$\hat{\mathcal{H}} = -\sum_{i}^{N} \varepsilon_i |i\rangle\langle i| + \sum_{i\neq j} w_{ij} |i\rangle\langle j|, \tag{7}$$

in which the recovery rates ε_i play the role of the on-site energies and the infection rates w_{ij} can be associated with the transfer (hopping) integrals. Both of these values are random and this makes the further analysis nontrivial even in the dilute regime. The topology of the underlying network of sites, in principle, can be arbitrary but the simplest choice is a regular D-dimensional lattice with nearest-neighbor interactions only. Furthermore, for simplicity, we consider a square lattice and thus the second sum in Eq. (7) runs for each site over $Z=4$ its nearest neighbors only. It is worth mentioning that if the on-site matrix elements satisfy the sum rule $\varepsilon_i=\Sigma_j w_{ij}$; then, the number of occupied sites is conserved and the problem is equivalent to the random walk problem on a lattice with random transition rates [21] or to the scalar vibrational problem for a lattice with force-constant disorder [22]. Notice also that decoupling of the single-site probabilities can also be made in the nondilute regime by assuming that $\bar{P}_{ij}=\bar{P}_i\bar{P}_j$—i.e., ignoring possible correlations in occupation of the communicating sites. This brings a nonlinearity to the problem which can be treated within the mean-field approach for ideal lattices [7].

III. SOLUTION

The formal solution of the problem given by Eq. (5) is straightforward,

$$|\bar{P}(t)\rangle = e^{\hat{\mathcal{H}}t}|\bar{P}(0)\rangle = \sum_{j} e^{\lambda_j t}\langle \mathbf{e}^j|\bar{P}(0)\rangle|\mathbf{e}^j\rangle, \tag{8}$$

where $|\mathbf{e}^j\rangle=|e_1^j,\ldots,e_N^j\rangle$ and λ_j are the eigenvectors and eigenvalues of the Hamiltonian, respectively, $\hat{\mathcal{H}}|\mathbf{e}^j\rangle=\lambda_j|\mathbf{e}^j\rangle$. Equivalently, this solution can be written via the Laplace transform of the state vector, $|\bar{P}(\lambda)\rangle=\int_0^\infty|\bar{P}(t)\rangle e^{-\lambda t}\mathrm{d}t$,

$$\begin{aligned}|\bar{P}(\lambda)\rangle &= (\lambda-\hat{\mathcal{H}})^{-1}|\bar{P}(0)\rangle \equiv \hat{\mathcal{G}}|\bar{P}(0)\rangle \\ &= \sum_{j}(\lambda-\lambda_j)^{-1}\langle \mathbf{e}^j\,|\bar{P}(0)\rangle|\mathbf{e}^j\rangle,\end{aligned} \tag{9}$$

where $\hat{\mathcal{G}}=(\lambda-\hat{\mathcal{H}})^{-1}$ is the resolvent operator.

We are interested in the time evolution of the total number of infected sites,

$$I(t) = \frac{1}{N}\left\langle \sum_{ii_0}^{N} \bar{P}_i(t;i_0)\right\rangle \equiv \frac{1}{N}\left\langle \sum_{ii_0}^{N}\langle i|\bar{P}(t;i_0)\rangle\right\rangle, \tag{10}$$

averaged over different realizations of disorder (angular brackets) and/or over initial conditions [for concreteness, a single site i_0 is infected at $t=0$—i.e., $\bar{P}_i(0;i_0)=\delta_{ii_0}$] and its Laplace transform,

$$I(\lambda) = \frac{1}{N}\sum_{ii_0}^{N}\langle \mathcal{G}_{ii_0}(\lambda)\rangle. \tag{11}$$

The other quantity of interest is the mean-squared displacement of the epidemic,

$$\langle R^2(t)\rangle = \frac{1}{N}\sum_{ii_0}^{N}\mathbf{R}_{i_0i}^2\langle \bar{P}_i(t;i_0)\rangle, \quad \langle R^2(\lambda)\rangle = \frac{1}{N}\sum_{ii_0}^{N}\mathbf{R}_{i_0i}^2\langle \mathcal{G}_{ii_0}(\lambda)\rangle, \tag{12}$$

where $\mathbf{R}_{i_0i}$ is the vector connecting site i_0 with site i.

As follows from Eq. (8) the dynamics of the system in the dilute regime is defined by the eigenspectrum of the Hamiltonian. The set of characteristic times (inverse eigenvalues) controls the evolution of the system with different eigenvalues being important for different time scales. The long-time dynamics of the system is defined by the maximum eigenvalue of the Hamiltonian, $\lambda_{\max}$ ($\lambda_{\max}<0$ in the dilute regime), and our aim is to find an estimate for $\lambda_{\max}$ and how it depends on the degree of disorder. The maximum eigenvalue depends on all the recovery and infection rates, $\lambda_{\max}(\varepsilon_i,w_{ij})$, and this obviously complicates its analytical evaluation. The exact analytical solution of the problem in the general case is not currently known and numerous approximate analytical (see, e.g., [20,23]) and numerical (see, e.g., [24,25]) methods have been developed for evaluation of the spectrum of disordered Hamiltonians. Below, we use one of the well-developed self-consistent mean-field approaches (the homomorphic cluster approximation within the coherent potential approximation [26,27]) to find the estimates for $\lambda_{\max}$ in the case of off-diagonal disorder and compare these results with the exact numerical calculations both for the Hamiltonian used in the approximate approach and for the original problem [cellular automaton (CA) calculations]. Before analyzing the disordered system, we start, however, with a trivial case of an ideal crystalline lattice in order to illuminate our approach.

A. Ideal lattice

In the case of an ideal crystalline lattice, the probability distribution functions are δ functions $\rho_\varepsilon(\varepsilon_i)=\delta(\varepsilon_i-\varepsilon_0)$ and $\rho_w(w_{ij})=\delta(w_{ij}-w_0)$ and the translationally invariant solutions of the eigenproblem are well known (see, e.g., [28]), so that the eigenvectors are the Bloch waves characterized by the wave vector $\mathbf{k}$,

$$|\mathbf{e}_\mathbf{k}\rangle = N^{-1/2}\sum_{i} e^{i\mathbf{k}\cdot\mathbf{R}_i}|i\rangle, \tag{13}$$

with $\mathbf{R}_i$ being the position vector of site i, and the eigenvalues are

$$\lambda(\mathbf{k}) = -\varepsilon_0 + w_0 S_\mathbf{k}, \tag{14}$$

where $S_\mathbf{k}=\Sigma_j e^{-i\mathbf{k}\cdot\mathbf{R}_{ij}}$ (the sum is taken over j running over the nearest neighbors to arbitrary site i) is the structure factor and the wave vector $\mathbf{k}$ lies in the first Brillouin zone of the reciprocal space so that $\lambda_{\max}=\lambda_{\mathbf{k}=0}=-\varepsilon_0+Zw_0$.

The Laplace transform of the total number of infected states is then [see Eq. (11)] $I(\lambda)=(\lambda-\lambda_{\mathbf{k}=0})^{-1}$, and thus

$$I(t) = e^{\lambda_{\mathbf{k}=0}t} = e^{(-\varepsilon_0+w_0Z)t}. \tag{15}$$

This means that in the dilute regime $\eta=w_0/\varepsilon_0\ll 1$, the exponent in Eq. (15) is negative and the total number of infected states decays exponentially with time.

Therefore, for an ideal crystalline lattice the critical value of the parameter $\eta = w_0/\varepsilon_0$ obtained from the equation $\lambda_{\max} = -\varepsilon_0 + Zw_0 = 0$ for the system described by the approximate master equation is

$$\eta^*_{\text{cryst}} = Z^{-1}, \tag{16}$$

which gives $\eta^*_{\text{cryst}} = 0.25$ for a square lattice with nearest-neighbor interactions only. This estimate is equivalent to the standard (not self-consistent) mean-field estimate and, as expected, is less than the true critical value, $\eta_{\text{cryst}} \simeq 0.4122$ [7].

The Laplace transform of the mean-squared displacement $\langle R^2(\lambda)\rangle$ for ideal crystal in the dilute regime is given by the expression [see Eq. (12)] $\langle R^2(\lambda)\rangle = w_0 a^2 Z(\lambda - \lambda_{\mathbf{k}=0})^{-2}$, with a being the nearest-neighbor distance, and thus

$$\langle R^2(t)\rangle = w_0 a^2 Z t e^{\lambda_{\mathbf{k}=0} t} = w_0 a^2 Z t e^{(-\varepsilon_0 + w_0 Z)t}. \tag{17}$$

It follows from Eq. (17) that the mean-squared displacement increases exponentially in the active state when $\eta > \eta^*_{\text{cryst}}$ (i.e., $\lambda_{\max} = \lambda_{\mathbf{k}=0} > 0$) and exponentially decays with time in absorbing state for $\eta < \eta^*_{\text{cryst}}$ (i.e., $\lambda_{\max} < 0$).

B. Disordered lattice

The problems become much harder for a disordered lattice characterized by random infection and recovery rates. In order to find the time dependence of the number of infected sites and the mean-squared displacement for the contact process we need to evaluate the configurationally averaged resolvent operator $\langle \hat{\mathcal{G}} \rangle$ [see Eqs. (9)–(12)]. This can be done approximately for lattice models with certain types of disorder: namely, with diagonal disorder (disorder in the recovery rates, ε_i), off-diagonal disorder (disorder in transfer rates, w_{ij}), and for binary systems with substitutional disorder (two species of sites randomly occupy the lattice sites [29]). One of the successful approximate analytical approaches is the self-consistent mean-field approach [coherent potential approximation (CPA)] which allows the main spectral features of the disordered Hamiltonian and its eigenfunctions to be modeled (see, e.g., [28]).

The main idea of the CPA is in replacement of the disordered lattice by the ideal crystalline one which is characterized by the effective complex parameters (complex fields)—e.g., by the effective recovery, $\tilde{\varepsilon}(\lambda) = \tilde{\varepsilon}'(\lambda) + i\tilde{\varepsilon}''(\lambda)$, and transmission, $\tilde{w}(\lambda) = \tilde{w}'(\lambda) + i\tilde{w}''(\lambda)$, rates which depend on the eigenvalues λ of the Hamiltonian and should be found self-consistently. The self-consistency equation follows from the requirement that a single defect placed in the effective crystal does not scatter the effective crystalline eigenfunctions if averaged over disorder.

In what follows, for concreteness, we consider the case of off-diagonal disorder, when all the recovery rates are the same, $\rho(\varepsilon_i) = \delta(\varepsilon_i - \varepsilon_0)$, while the transfer rates are taken from a uniform (box) distribution,

$$\rho(w_{ij}) = \begin{cases} (2\Delta)^{-1} & \text{if } w_0 - \Delta \leqslant w_{ij} \leqslant w_0 + \Delta, \\ 0 & \text{otherwise}, \end{cases} \tag{18}$$

where Δ is the half-width of the distribution, $0 \leqslant \Delta \leqslant w_0$, and the mean value $\bar{w}_{ij}$ coincides with the crystalline one, $\bar{w}_{ij} = w_0$. The particular form of the distribution (18) is not important for the method discussed below. The conclusions are also applicable to any well-behaved distribution given that the mean value coincides with the value for the ordered system.

The disordered Hamiltonian (7) can be conveniently rewritten in the bond representation [22]

$$\hat{\mathcal{H}} = \sum_{(ij)} \left(-Z^{-1}\varepsilon_i |i\rangle\langle i| - Z^{-1}\varepsilon_j |j\rangle\langle j| + w_{ij}|i\rangle\langle j| + w_{ji}|j\rangle\langle i|\right), \tag{19}$$

where the summation is taken over all bonds (ij) in the system. Such a form of the Hamiltonian allows the single noncorrelated scatterers (bonds) to be introduced in the absence of the on-site disorder (the homomorphic cluster approximation [26,27]). The next step is to replace the above Hamiltonian with the effective non-Hermitian one,

$$\hat{\tilde{\mathcal{H}}} = \sum_{(ij)} \left(-Z^{-1}\tilde{\varepsilon} |i\rangle\langle i| - Z^{-1}\tilde{\varepsilon} |j\rangle\langle j| + \tilde{w}|i\rangle\langle j| + \tilde{w}|j\rangle\langle i|\right), \tag{20}$$

where the effective fields $\tilde{\varepsilon}$ and $\tilde{w}$ are found from the following two self-consistency equations (see Appendix A) [30]:

$$\left\langle \frac{Z^{-1}(\tilde{\varepsilon} - \varepsilon_0) \pm (w_{ij} - \tilde{w})}{1 - (\tilde{\mathcal{G}}_{ii} \pm \tilde{\mathcal{G}}_{ij})(Z^{-1}(\tilde{\varepsilon} - \varepsilon_0) \pm (w_{ij} - \tilde{w}))} \right\rangle = 0. \tag{21}$$

The averaging in Eqs. (21) is performed over random values of transition rates w_{ij} distributed according to the probability distribution given by Eq. (18). The effective resolvent (Green's function) elements $\mathcal{G}_{ii}$ and $\mathcal{G}_{ij}$ can be expressed via the ideal crystalline resolvent elements $\mathcal{G}^{\text{cryst}}_{ii}$ of complex argument (see Appendix A),

$$\tilde{\mathcal{G}}_{ii}(\lambda) = \frac{w_0}{\tilde{w}} \mathcal{G}^{\text{cryst}}_{ii}\left(\frac{w_0}{\tilde{w}}(\lambda + \tilde{\varepsilon}) - \varepsilon_0\right), \tag{22}$$

$$\tilde{\mathcal{G}}_{ij}(\lambda) = \frac{1}{Z\tilde{w}}[(\lambda + \tilde{\varepsilon})\tilde{\mathcal{G}}_{ii}(\lambda) - 1],$$

which are well known for the square lattice (see, e.g., [28]).

The self-consistency equations (21) can be solved numerically and thus both effective fields can be found. Once the complex effective fields $\tilde{\varepsilon}(\lambda)$ and $\tilde{w}(\lambda)$ are known, then the spectrum of the effective Hamiltonian can be found (see Fig. 1), enabling the dynamics of the system in the dilute regime within the self-consistent mean-field approach to be studied.

It can be shown that the total number of infected states and the mean-squared displacement in the CPA obey the equations (see Appendix B)

$$I(t) = -\frac{1}{\pi} \operatorname{Im} \int_{\lambda_{\min}(\Delta)}^{\lambda_{\max}(\Delta)} \frac{e^{\lambda t}}{\lambda - \tilde{\lambda}(\lambda, \mathbf{k} = 0)} d\lambda$$
$$= -\frac{1}{\pi} \operatorname{Im} \int_{\lambda_{\min}(\Delta)}^{\lambda_{\max}(\Delta)} \frac{e^{\lambda t}}{\lambda + \tilde{\varepsilon}(\lambda) - Z\tilde{w}(\lambda)} d\lambda \tag{23}$$

and

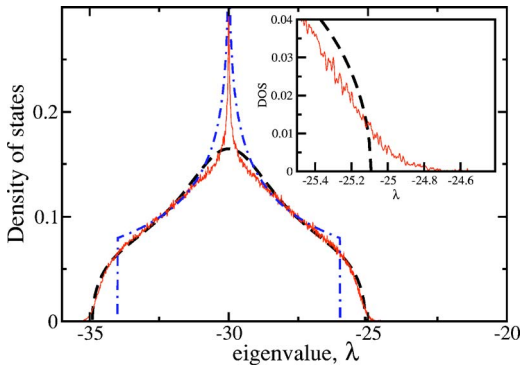

FIG. 1. (Color online) The spectrum of the effective (dashed line) and true (solid line) Hamiltonian (density of states) defined on the square lattice with nearest-neighbor interactions ($Z=4$) in the system with transmission rates uniformly distributed around the mean value $w_0=1$ with half-width $\Delta=1.0$ and $\varepsilon_0=30$. The exact spectrum was obtained numerically using the kernel polynomial method [31] for a model of $N=2000\times2000$ sites. The spectrum of the crystalline Hamiltonian with all nearest-neighbor interactions ($\Delta=0$) is shown by the dot-dashed line. The inset magnifies the spectrum around the top of the band.

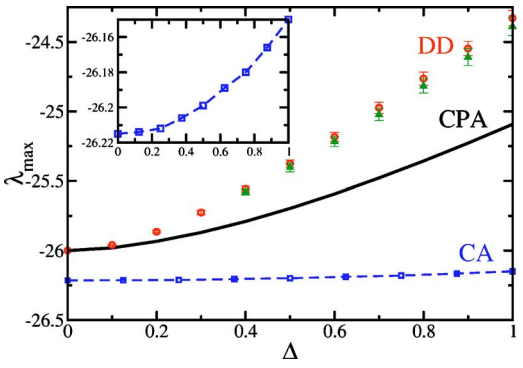

FIG. 2. (Color online) The dependence of the maximum eigenvalue $\lambda_{\max}$ evaluated using a mean-field approach (solid curve, labeled CPA) and $\lambda^*_{\max}$ calculated by direct diagonalization (DD, circles for 4000×4000 and triangles for 2000×2000 lattices; the error bars represent the standard deviations of the distribution of the maximum eigenvalues) on the degree of disorder characterized by the half-width of the box distribution Δ for $\varepsilon_0=30$ and $w_0=1$. The squares (labeled CA) represent the long-time decay rates λ_{CA} obtained by the CA simulations, each data point corresponding to approximately 5×10^{10} runs, on a 5×5 lattice. The inset shows a version of the CA data scaled vertically to clarify the trend.

$$\langle R^2(t)\rangle = -\frac{1}{\pi}\,\mathrm{Im}\int_{\lambda_{\min}(\Delta)}^{\lambda_{\max}(\Delta)} e^{\lambda t}\left[\frac{\nabla_{\mathbf{k}}^2\tilde{\varepsilon}(\lambda,\mathbf{k})}{[\lambda-\tilde{\lambda}(\lambda,\mathbf{k})]^2}\right]_{\mathbf{k}=0} d\lambda$$
$$= -\frac{1}{\pi}\,\mathrm{Im}\int_{\lambda_{\min}(\Delta)}^{\lambda_{\max}(\Delta)} \frac{Za^2\tilde{w}(\lambda)e^{\lambda t}}{[\lambda+\tilde{\varepsilon}(\lambda)-Z\tilde{w}(\lambda)]^2} d\lambda, \quad (24)$$

with the effective dispersion law

$$\tilde{\lambda}(\lambda,\mathbf{k}) = -\tilde{\varepsilon}(\lambda)+\tilde{w}(\lambda)S_{\mathbf{k}}. \quad (25)$$

The integration in Eqs. (23) and (24) is performed over the band(s) of eigenvalues, $\lambda_{\min}(\Delta)\leqslant\lambda\leqslant\lambda_{\max}(\Delta)$, where the imaginary parts of the effective fields are finite for $\Delta>0$.

As follows from Eqs. (23) and (24) the long-time dynamics of the system both for the number of infected nodes $I(t)$ and for the mean-squared displacement $\langle R^2(t)\rangle$ are defined by the largest eigenvalue. The upper band edge $\lambda_{\max}(\Delta)$ can be found within the CPA from the self-consistency equations (21) by solving them for $\lambda>\lambda_{\max}(\Delta)$ where both effective fields are real—i.e., $F_{\pm}(\tilde{w}',\tilde{\varepsilon}',\lambda)=0$ with $F_{\pm}$ standing for the left-hand side of Eqs. (21). The analysis of the dependences of the effective fields on λ shows that the upper band edge corresponds to the branching point at which the following equation holds (see Appendix C):

$$\left[\frac{\partial F_+}{\partial\tilde{w}'}\frac{\partial F_-}{\partial\tilde{\varepsilon}'}-\frac{\partial F_-}{\partial\tilde{w}'}\frac{\partial F_+}{\partial\tilde{\varepsilon}'}\right]_{\lambda_{\max}(\Delta)}=0. \quad (26)$$

The solution of Eq. (26) simultaneously with the self-consistency equations (21) allows the position of the upper band edge, $\lambda_{\max}(\Delta)$, to be found. The results of such an analysis are shown in Fig. 2 (see the solid line) for a particular choice of parameter $\eta\ll\eta^*_{\mathrm{cryst}}\sim1$. When all the transfer rates are the same ($\Delta=0$), the maximum value coincides with the crystalline upper band edge, $\lambda_{\max}/w_0=-\eta^{-1}+Z$. When the disorder is introduced to the system the upper band edge shifts to larger values of λ and thus the long-time dynamics slows down. The value of the shift increases with increasing degree of disorder characterized by the value of Δ (see Fig. 2). This is a general effect that is independent of the type and form (probability distribution functions) of disorder given that the mean values of random parameters are the same as for the ordered system. Indeed, any disorder brought to the system is equivalent to introducing additional interactions between the ordered eigenstates which unavoidably result in the level-repelling effect for the bare (crystalline) eigenstates [32] that is to the broadening of the spectrum. Therefore the disorder-induced slowing down of the dynamics of the contact process in the dilute regime is a general effect (if disorder does not influence the mean values of random variables).

It is known that the spectrum of the Hamiltonian obtained within the self-consistent mean-field approach usually reproduces very well the main features of the spectrum of the Hamiltonian (see Fig. 1) excluding some special points like singularities (e.g., the midband singularity) and band edges (see the inset in Fig. 1). For the eigenstates around the band edges, the fluctuations of random parameters are essential and they lead to strong localization of the eigenstates around the band edges. In fact, the true (non-mean-field) density of states shows exponentially decaying band tails instead of sharp band edges typical for the mean-field crystals (see the inset in Fig. 1). The mean-field approach does not take into account such fluctuations and thus the mean-field value of $\lambda_{\max}$ is only the (low-bound) estimate of the true maximum eigenvalue of the Hamiltonian, $\lambda^*_{\max}$. The values of $\lambda^*_{\max}$ are random values depending on a particular realization of disorder. We have calculated numerically (using the Lanczos method) the distributions of the maximum eigenvalues for system of different sizes (up to $N=4000\times4000$ sites) and different values of Δ. The results for $\langle\lambda^*_{\max}(\Delta)\rangle$ (averaged over 500 disorder realizations) are shown in Fig. 2. The av-

eraged maximum eigenvalue depends on N (see Fig. 2) apparently approaching some limiting value which is certainly less than the band edge, $-\varepsilon_0+Zw$, for a crystal with all transfer rates equal to $w=w_0+\Delta$.

IV. DISCUSSION

The main finding from our analysis is that the disorder slows down the dynamics of the contact process in the dilute regime when the system is far in the absorbing state given that the mean values of the random parameters are the same as for the ordered system. This conclusion is supported by the exact solution for the contact process using the cellular automaton simulations which were performed using a continuous-time algorithm similar to the n-fold way (see, e.g., [33]). The CA simulations were used for evaluation of the inverse decay time for $I(t\to\infty)$ (see squares in Fig. 2) which can be compared with $\lambda_{\max}$ (solid line) and $\lambda^{*}_{\max}$ (circles and triangles in Fig. 2).

First, we compare the approximate (CPA) long-time decay rate (magnitude of the maximum eigenvalue) with the exact (CA) one for an ideal (ordered) lattice. The dilute regime approximation enhances the epidemic and thus results in smaller long-time decay rates for $I(t)$ and $\langle R^2(t)\rangle$. Indeed, as follows from Fig. 2 for $\Delta=0$, the exact value λ_{CA} ($\simeq -26.215$ for a particular typical choice of parameters, $\varepsilon_0=30$ and $w_0=1$) is smaller than the approximate one, $\lambda_{\max}=-\varepsilon+Zw_0=-26$. When disorder is incorporated in the system the approximate decay rate decreases (eigenvalue increases) with increasing disorder (see the solid line in Fig. 2). The exact value of the decay rate in the disordered system also decreases (λ_{CA} increases; see the inset in Fig. 2) with increasing disorder, thus confirming the tendency found in the dilute approximation, although the increase in λ_{CA} is appreciably smaller than the increase in $\lambda_{\max}$ and/or $\lambda^{*}_{\max}$.

The value of the decrease in the decay rate with increasing disorder, being proportional to the width of the tail, $|\lambda_{\max}(\Delta=0)-\lambda_{\max}(\Delta=w_0)|/w_0 \sim |\lambda_{\max}(\Delta=0)-\lambda^{*}_{\max}(\Delta=w_0)|/w_0 \sim 0.1$, is naturally small due to the assumptions made; i.e., the system is far in the absorbing state. However, the sign of the effect is important and it cannot be predicted by the standard (not-self-consistent) mean-field analysis for the contact processes [7] if the mean values in the disordered system coincide with those for the ordered one. The other comment concerns the dependence of the effect on the parameters of the system. The broadening of the spectrum of the Hamiltonian does not depend on the mean recovery rate ε_0. This means that if ε_0 increases, then the absolute magnitude of the effect within the CA treatment, $\lambda_{\mathrm{CA}}(\Delta=0)-\lambda_{\mathrm{CA}}(\Delta=w_0)$, tends to $\lambda_{\max}(\Delta=0)-\lambda^{*}_{\max}(\Delta=w_0)$. If the recovery rate decreases, the system approaches the active state and approximations made for the dilute regime break down. Therefore the analysis performed cannot be considered as a good approximation around criticality. In fact, as follows from the preliminary CA analysis, the value of $\lambda_{\mathrm{CA}}(\Delta=0)-\lambda_{\mathrm{CA}}(\Delta=w_0)$ increases with decreasing ε_0 and can reach zero around criticality and even change sign (to be discussed further elsewhere); i.e., the introduction of disorder into a crystalline system at criticality causes a transition to the absorbing state rather than further into the active phase.

The last comment concerns a possible rough estimate of the critical parameter η_c for transition from the absorbing to active state in disordered system. This estimate can be found by solving the equation $\lambda_{\max}(\Delta)=0$ [or $\lambda^{*}_{\max}(\Delta)=0$], which gives, $\eta_c \simeq \eta_c^{\mathrm{cryst}}\{1+[\lambda_{\max}(\Delta=0)-\lambda_{\max}(\Delta=w_0)]/w_0\}$. Of course, the quality of this estimate is the same as that for the crystal—i.e., $\eta_c^{\mathrm{cryst}}=Z^{-1}=0.25$ as compared to exact value $\eta_c \simeq 0.4122$—and can serve only as a reliable low bound for the critical value.

V. CONCLUSIONS

We have presented the analysis of the contact process in the limit of low density of occupied (infected) sites [see Eq. (4)]—i.e., in the dilute regime for the infected sites when all the correlation effects in occupation probabilities can be ignored. This limit occurs, e.g., when the transfer rate is much smaller than the infection rate, $w \ll \varepsilon$. The system resides in the absorbing state for such a range of parameters and its dynamics can be described by using the quantum-mechanical tight-binding Hamiltonian. The disorder, in both the transfer and recovery rates, can be incorporated into the formulation which can be reduced to the eigenproblem for the Anderson-like Hamiltonian [see Eq. (7)]. The eigenproblem can be solved approximately analytically (self-consistent mean field) and exactly numerically, and thus the estimate of the decay rate $|\lambda_{\max}|$ for long-time dynamics can be found for different degrees of disorder (see Fig. 2). The approximate solution is supported by exact numerical analysis using the cellular automaton approach. In particular, we conclude that any type of disorder which does not change the mean values of random parameters slows down the long-time dynamics of the contact process occurring in the far-absorbing state.

APPENDIX A: SELF-CONSISTENCY EQUATION WITHIN THE HOMOMORPHIC CLUSTER CPA

In this appendix, we derive the matrix self-consistency equation within the homomorphic cluster CPA. Within the self-consistent mean-field approach the disordered lattice is replaced by an ideal lattice characterized by self-consistently found effective complex parameters (fields): namely, by the effective recovery and transmission rates $\tilde{\varepsilon}(\lambda)$ and $\tilde{w}(\lambda)$. The effective Hamiltonian describing this effective lattice is given by Eq. (20). The effective fields are found within the single-defect approximation according to the following standard procedure [28,29]. A single defect bond (ij) taken from the random set of bonds characterizing the disordered lattice is placed in the effective medium. The single-defect Hamiltonian $\hat{\tilde{\mathcal{H}}}_1$ is the sum of the ideal effective Hamiltonian and the perturbation due to the defect bond, $\hat{\tilde{\mathcal{H}}}_1=\hat{\tilde{\mathcal{H}}}+\delta\hat{V}$, where

$$\delta\hat{V}=-Z^{-1}[\varepsilon_0-\tilde{\varepsilon}(\lambda)](|i\rangle\langle i|+|j\rangle\langle j|)+[w_{ij}-\tilde{w}(\lambda)](|i\rangle\langle j|+|j\rangle\langle i|). \tag{A1}$$

This defect bond influences (scatters) the eigenfuctions of

the original effective Hamiltonian. In the CPA, the effective medium is tuned in such a manner that this scattering vanishes on average. In other words, the single-defect scattering operator $\hat{T}$, introduced by the equation $\hat{T}=\delta\hat{V}+\delta\hat{V}\hat{\tilde{\mathcal{G}}}\hat{T}$ [where $\hat{\tilde{\mathcal{G}}}=(\lambda-\hat{\tilde{\mathcal{H}}})^{-1}$ is the effective resolvent], averaged over different realizations of defect bond taken from the same probability distribution as for a disordered medium should be zero—i.e.,

$$\langle\hat{T}\rangle=\langle\delta\hat{V}(1-\tilde{\mathcal{G}}\delta\hat{V})^{-1}\rangle=0. \tag{A2}$$

The above equation is the self-consistency matrix equation where the scattering matrix in the site basis is

$$\hat{T}=\frac{1}{|1-\tilde{\mathcal{G}}\delta\hat{V}|}\begin{pmatrix}\delta\varepsilon+(\delta w^2-\delta\varepsilon^2)\tilde{\mathcal{G}}_{jj} & \delta w-(\delta w^2-\delta\varepsilon^2)\tilde{\mathcal{G}}_{ij}\\ \delta w-(\delta w^2-\delta\varepsilon^2)\tilde{\mathcal{G}}_{ji} & \delta\varepsilon+(\delta w^2-\delta\varepsilon^2)\tilde{\mathcal{G}}_{jj}\end{pmatrix}, \tag{A3}$$

with $\delta\varepsilon=-Z^{-1}[\varepsilon_0-\tilde{\varepsilon}(\lambda)]$ and $\delta w=w_{ij}-\tilde{w}(\lambda)$. Bearing in mind that $\tilde{\mathcal{G}}_{ii}=\tilde{\mathcal{G}}_{jj}$ and $\tilde{\mathcal{G}}_{ij}=\tilde{\mathcal{G}}_{ji}$ the scattering matrix can be easily diagonalized by a similarity transformation to a new basis, so that

$$\hat{T}=\begin{pmatrix}\dfrac{\delta\varepsilon-\delta w}{1-(\tilde{\mathcal{G}}_{ii}-\tilde{\mathcal{G}}_{ij})(\delta\varepsilon-\delta w)} & 0\\ 0 & \dfrac{\delta\varepsilon+\delta w}{1-(\tilde{\mathcal{G}}_{ii}+\tilde{\mathcal{G}}_{ij})(\delta\varepsilon+\delta w)}\end{pmatrix}, \tag{A4}$$

which straightforwardly results in Eq. (21).

The elements of the scattering matrix $\hat{T}$ depend on the diagonal and off-diagonal matrix elements of the effective resolvent, $\tilde{\mathcal{G}}_{ii}$ and $\tilde{\mathcal{G}}_{ij}$, respectively. The effective Hamiltonian describes the ideal lattice characterized by complex parameters $\tilde{\varepsilon}$ and $\tilde{w}$, and thus its eigenfuctions are the Bloch waves given by Eq. (13) with effective dispersion described by Eq. (25). This allows the real-space matrix elements of the resolvent to be expressed via the reciprocal-space ones and then, via similar elements of the resolvent for ideal crystalline lattice,

$$\begin{aligned}\tilde{\mathcal{G}}_{ii}(\lambda)&=\frac{1}{N}\sum_{\mathbf{k}}\frac{1}{\lambda+\tilde{\varepsilon}-\tilde{w}S_{\mathbf{k}}}\\&=\frac{w}{\tilde{w}N}\sum_{\mathbf{k}}\frac{1}{\lambda w/\tilde{w}+\tilde{\varepsilon}w/\tilde{w}-\varepsilon_0-\lambda_{\mathrm{cryst}}(\mathbf{k})}\\&=\frac{w}{\tilde{w}}\mathcal{G}_{ii}^{\mathrm{cryst}}\left[\frac{w(\lambda+\tilde{\varepsilon})}{\tilde{w}}-\varepsilon_0\right],\end{aligned} \tag{A5}$$

with $\mathcal{G}_{ii}^{\mathrm{cryst}}(\lambda)=N^{-1}\Sigma_{\mathbf{k}}[\lambda-\lambda_{\mathrm{cryst}}(\mathbf{k})]^{-1}$ being the crystalline resolvent characterized by the crystalline dispersion, $\lambda_{\mathrm{cryst}}(\mathbf{k})$, given by Eq. (14), and

$$\begin{aligned}\tilde{\mathcal{G}}_{ij}(\lambda)&=\frac{1}{N}\sum_{\mathbf{k}}\frac{e^{-i\mathbf{k}\mathbf{R}_{ij}}}{\lambda-\tilde{\lambda}(\lambda,\mathbf{k})}=\frac{1}{\tilde{w}ZN}\sum_{\mathbf{k}}\left(\frac{\lambda+\tilde{\varepsilon}}{\lambda-\tilde{\lambda}(\lambda,\mathbf{k})}-1\right)\\&=\frac{\lambda+\tilde{\varepsilon}}{\tilde{w}Z}\frac{1}{N}\sum_{\mathbf{k}}\frac{1}{\lambda-\tilde{\lambda}(\lambda,\mathbf{k})}-\frac{1}{\tilde{w}Z},\end{aligned} \tag{A6}$$

where $N^{-1}\Sigma_{\mathbf{k}}[\lambda-\tilde{\lambda}(\lambda,\mathbf{k})]^{-1}=\tilde{\mathcal{G}}_{ii}(\lambda)$. Equations (A5) and (A6) justify the expressions for the matrix elements of the effective resolvent given by Eq. (22).

APPENDIX B: NUMBER OF INFECTED SITES WITHIN THE CPA

The aim of this appendix is to derive Eq. (23) for the number of infected sites as a function of time. It is convenient to find the Laplace transform $I(\lambda)$ of the function $I(t)$ and then use the inverse transform

$$I(t)=\frac{1}{2\pi i}\int_{\delta-i\infty}^{\delta+i\infty}e^{\lambda t}I(\lambda)d\lambda \tag{B1}$$

to reveal Eq. (23). The Laplace transform $I(\lambda)$ is given by Eq. (11) in which, within the CPA, the averaged resolvent matrix element should be replaced by the matrix element of the effective resolvent,

$$I(\lambda)=\frac{1}{N}\sum_{ii_0}^{N}\tilde{\mathcal{G}}_{ii_0}(\lambda)=\frac{1}{N}\sum_{ii_0}^{N}\frac{1}{N}\sum_{\mathbf{k}}\frac{e^{-i\mathbf{k}\cdot\mathbf{R}_{ii_0}}}{\lambda-\tilde{\lambda}(\lambda,\mathbf{k})}. \tag{B2}$$

Bearing in mind the identity $\Sigma_i e^{-i\mathbf{k}\cdot\mathbf{R}_{ii_0}}=N\delta_{\mathbf{k},0}$, we obtain $I(\lambda)=(\lambda-\tilde{\lambda}_{\mathbf{k}=0})^{-1}$. Substitution of this expression into Eq. (B1) gives

$$I(t)=\frac{1}{2\pi i}\int_{\delta-i\infty}^{\delta+i\infty}\frac{e^{\lambda t}}{\lambda-\tilde{\lambda}_{\mathbf{k}=0}}d\lambda. \tag{B3}$$

The effective dispersion $\tilde{\lambda}_{\mathbf{k}}$ depends on the the effective fields $\tilde{w}(\lambda)$ and $\tilde{\varepsilon}(\lambda)$ which are analytic functions of λ everywhere except the finite interval on the real axis (branch cut), $\lambda\in[\lambda_{\min},\lambda_{\max}]$, where the density of states of the effective Hamiltonian is finite (see, e.g., [34] and references therein). The contour of integration in Eq. (B3) can be transformed into a closed one around the branch cut and thus, taking into account that the real part of the integrand is a continuous function through the branch cut but the imaginary part changes sign, Eq. (23) follows from Eq. (B3) and Eq. (24) can be derived in a similar fashion.

APPENDIX C: EQUATION FOR THE BAND EDGE

The two self-consistency equations (21) can be recast in the following form:

$$\int_0^\infty\frac{\delta\varepsilon-\delta w}{1-(\tilde{\mathcal{G}}_{ii}-\tilde{\mathcal{G}}_{ij})(\delta\varepsilon-\delta w)}\rho(w_{ij})dw_{ij}\equiv F_-(\tilde{\varepsilon},\tilde{w},\lambda)=0, \tag{C1}$$

$$\int_0^\infty \frac{\delta\varepsilon + \delta w}{1 - (\tilde{\mathcal{G}}_{ii} + \tilde{\mathcal{G}}_{ij})(\delta\varepsilon + \delta w)} \rho(w_{ij}) \mathrm{d}w_{ij} \equiv F_+(\tilde{\varepsilon}, \tilde{w}, \lambda) = 0. \tag{C2}$$

For any value of λ in the complex plane, these equations can be solved and two complex fields $\tilde{\varepsilon}(\lambda)$ and $\tilde{w}(\lambda)$ can be found. On the real axis for λ, $\lambda \geqslant \lambda_{\max}$, both fields are also real, $\tilde{\varepsilon}(\lambda) = \tilde{\varepsilon}'(\lambda)$ and $\tilde{w}(\lambda) = \tilde{w}'(\lambda)$, with $\lambda_{\max}$ being the branching point. In this range of λ, it is convenient to rewrite Eqs. (C1) and (C2) in the following form:

$$\begin{cases} \tilde{\varepsilon}' & = \varepsilon_-(\tilde{w}', \lambda), \\ \tilde{\varepsilon}' & = \varepsilon_+(\tilde{w}', \lambda), \end{cases} \tag{C3}$$

where $\varepsilon_{\mp}$ are multivalued functions of $\tilde{w}'$ for fixed λ. If $\lambda > \lambda_{\max}$, these contour lines usually cross at two points one of which corresponds to the physical solution. At the branching point $\lambda = \lambda_{\max}$, these two solutions merge and the condition for this is

$$\frac{\partial \varepsilon_-}{\partial \tilde{w}'} = \frac{\partial \varepsilon_+}{\partial \tilde{w}'}, \tag{C4}$$

which together with Eqs. (C1) and (C2) or with Eqs. (C3) allows the location of the upper band, $\lambda_{\max}$, to be found. Eq. (C4) can be rewritten in the more elegant but equivalent form given by Eq. (26). Indeed, differentiation of Eqs. (C1) and (C2) with respect to $\tilde{w}'$ gives

$$\frac{\partial \varepsilon_{\mp}}{\partial \tilde{w}'} = -\frac{\partial F_{\mp}}{\partial \tilde{w}'} \left(\frac{\partial F_{\mp}}{\partial \tilde{\varepsilon}'} \right)^{-1}, \tag{C5}$$

from which Eq. (26) follows straightforwardly with the use of Eq. (C4).

[1] H. Hinrichsen, Adv. Phys. **49**, 815 (2000).
[2] G. Ódor, Rev. Mod. Phys. **76**, 663 (2004).
[3] S. Dorogovtsev and J. Mendes, Adv. Phys. **51**, 1079 (2002).
[4] R. Albert and A.-L. Barabáshi, Rev. Mod. Phys. **74**, 47 (2002).
[5] M. J. Keeling and C. A. Gilligan, Nature (London) **407**, 903 (2000).
[6] B. Dybiec, A. Kleczkowski, and C. A. Gilligan, Phys. Rev. E **70**, 066145 (2004).
[7] J. Marro and R. Dickman, *Nonequilibrium Phase Transitions in Lattice Models* (Cambridge University Press, Cambridge, England, 1999).
[8] T. M. Liggett, *Interacting Particle Systems* (Springer-Verlag, New York, 1985).
[9] A. J. Noest, Phys. Rev. Lett. **57**, 90 (1986).
[10] M. Bramson, R. Durrett, and R. H. Schonmann, Ann. Prob. **19**, 960 (1991).
[11] A. G. Moreira and R. Dickman, Phys. Rev. E **54**, R3090 (1996).
[12] M. Vendruscolo and M. Marsili, Phys. Rev. E **54**, R1021 (1996).
[13] R. Cafiero, A. Gabrielli, and M. Munoz, Phys. Rev. E **57**, 5060 (1998).
[14] G. Szabó, H. Gergely, and B. Oborny, Phys. Rev. E **65**, 066111 (2002).
[15] J. Hooyberghs, F. Iglói, and C. Vanderzande, Phys. Rev. Lett. **90**, 100601 (2003).
[16] J. Hooyberghs, F. Iglói, and C. Vanderzande, Phys. Rev. E **69**, 066140 (2004).
[17] T. Vojta, Phys. Rev. E **70**, 026108 (2004).
[18] R. Dickman and A. G. Moreira, Phys. Rev. E **57**, 1263 (1998).
[19] H. K. Janssen, Phys. Rev. E **55**, 6253 (1997).
[20] B. Kramer and A. MacKinnon, Rep. Prog. Phys. **56**, 1469 (1993).
[21] J. Rudnick and G. Gaspari, *Elements of the Random Walk* (Cambridge University Press, Cambridge, England, 2004).
[22] S. N. Taraskin and S. R. Elliott, J. Phys.: Condens. Matter **14**, 3143 (2002).
[23] A. D. Mirlin, Phys. Rep. **326**, 259 (2000).
[24] *Computational Physics*, edited by K. H. Hoffmann and M. Schreiber (Springer Verlag, 1996).
[25] R. A. Römer and M. Schreiber, in *The Anderson Transition and its Ramifications—Localisation, Quantum Interference, and Interactions*, edited by T. Brandes and S. Kettemann (Springer, Berlin, 2003), pp. 3–19.
[26] F. Yonezawa and T. Odagaki, J. Phys. Soc. Jpn. **47**, 388 (1979).
[27] Q. Li, C. M. Soukoulis, and E. N. Economou, Phys. Rev. B **37**, 8289 (1988).
[28] E. N. Economou, *Green's Functions in Quantum Physics*, 2nd ed. (Springer, Heidelberg, 1983).
[29] H. Ehrenreich and L. Schwarts, Solid State Phys. **31**, 149 (1976).
[30] K. C. Chang and T. Odagaki, Phys. Rev. B **35**, 2598 (1987).
[31] R. N. Silver and H. Röder, Phys. Rev. E **56**, 4822 (1997).
[32] S. N. Taraskin, Y. L. Loh, G. Natarajan, and S. R. Elliott, Phys. Rev. Lett. **86**, 1255 (2001).
[33] J. A. McNeil and C. E. Price, Phys. Rev. B **50**, 1057 (1994).
[34] A. Gonis and J. W. Garland, Phys. Rev. B **16**, 1495 (1977).